Optimum RF stabilization of NTMs in large tokamaks

Richard Nies, Allan H. Reiman, Nathaniel J. Fisch

Princeton Plasma Physics Laboratory, Princeton University

Acknowledgements: Rob La Haye, Francesco Volpe

Theory and Simulation of Disruptions Workshop, PPPL/IAEA, July 22nd 2021

https://arxiv.org/abs/2106.06581

Motivation

Why stabilize Neoclassical Tearing Modes (NTMs)?

Degrade confinement and cause disruptions.

Typical NTM Life Cycle:

Rotate with plasma when born, then brake until they lock in lab frame.

How to stabilize NTMs?

Drive current at island O-point using RF.

When to stabilize NTMs?

In present-day devices: locking occurs at large width, quickly followed by disruption ⇒ stabilize during rotating phase. Focus of almost all experimental and theoretical studies.

Is this the best strategy for future larger devices?

The case for Locked Mode stabilization

In large devices, in particular ITER…

… Rotating island stabilization is challenging, may not be viable

Fast mode locking + RF broadening

… Locked modes do not have to be avoided at all cost

Small w_{lock} and large $\tau_M \Rightarrow$ no immediate disruption or loss of H-mode

… It might be preferable to stabilize locked instead of rotating modes

Higher η_{stab} & small $w_{\text{lock}} \Rightarrow$ lower peak RF power

Not limited by fast locking or large $w_{\text{seed}} \Rightarrow$ more robust

RF power does not need to be always on $\Rightarrow$ lower average RF power

Challenge 1: fast mode locking

High plasma inertia + small torque

$\Rightarrow$ small rotation - ITER: $f_{2/1} \sim 0.42$ kHz

$\Rightarrow$ fast locking - ITER (with blanket [1]):

$t_{\text{lock}} \sim 1.7$ s with $w_{\text{lock}} \sim 4.5\,\%\,a$

Must stabilize island below $w_{\text{crit}} \sim 2 - 3\,\%\,a$ [1], above which island slows and locks.

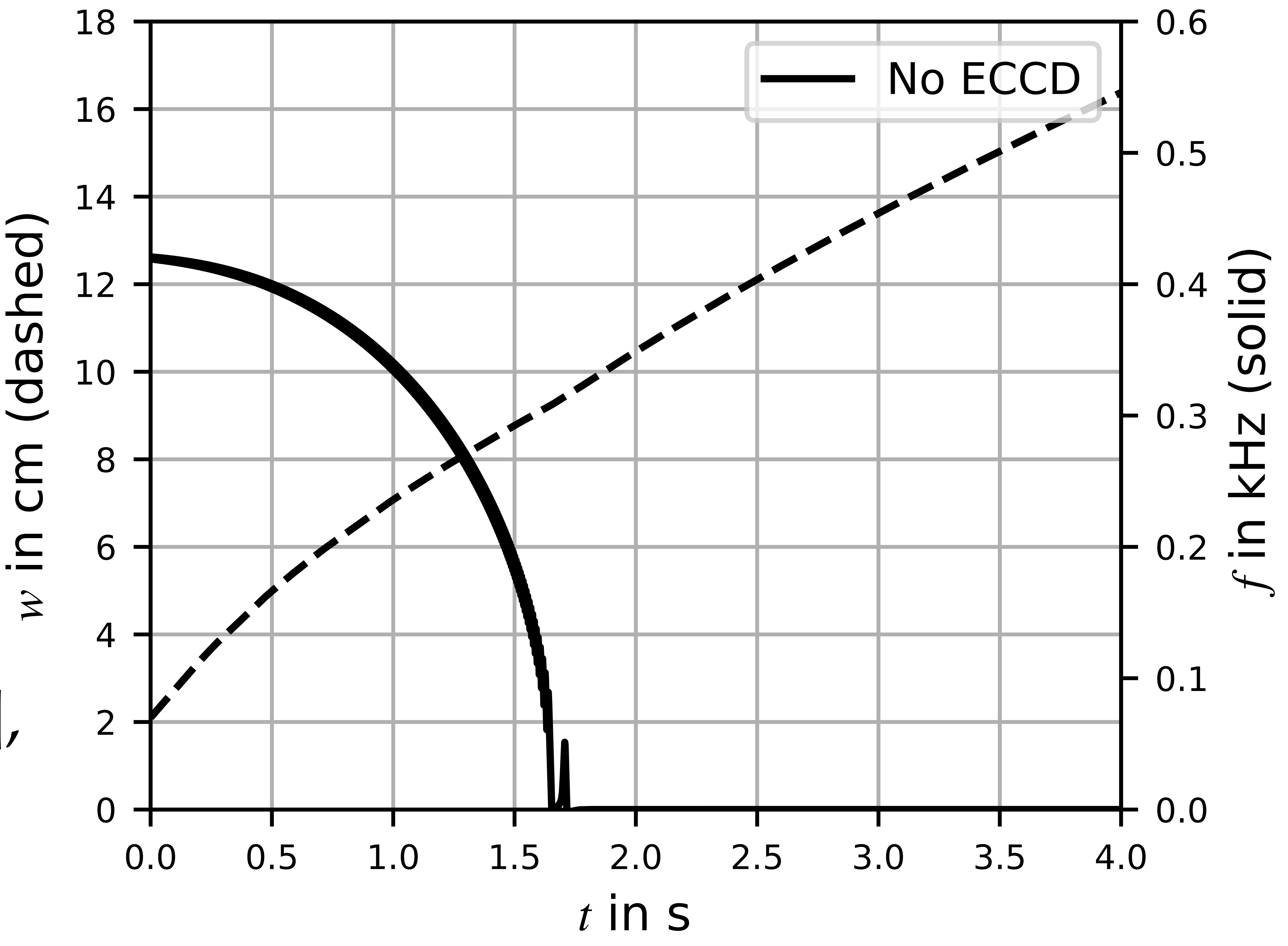

Make use of fast locking: stabilize **small** locked mode

[1] La Haye et al. 2017

Challenge 2: RF broadening

Stabilization efficiency **sensitive to broadening and misalignment**

Large EC broadening predicted due to edge density fluctuations (e.g. DIII-D [2])

ITER: broadening by factor 2.5-3.5 [3]

Plot of local stabilization efficiency η_{stab}

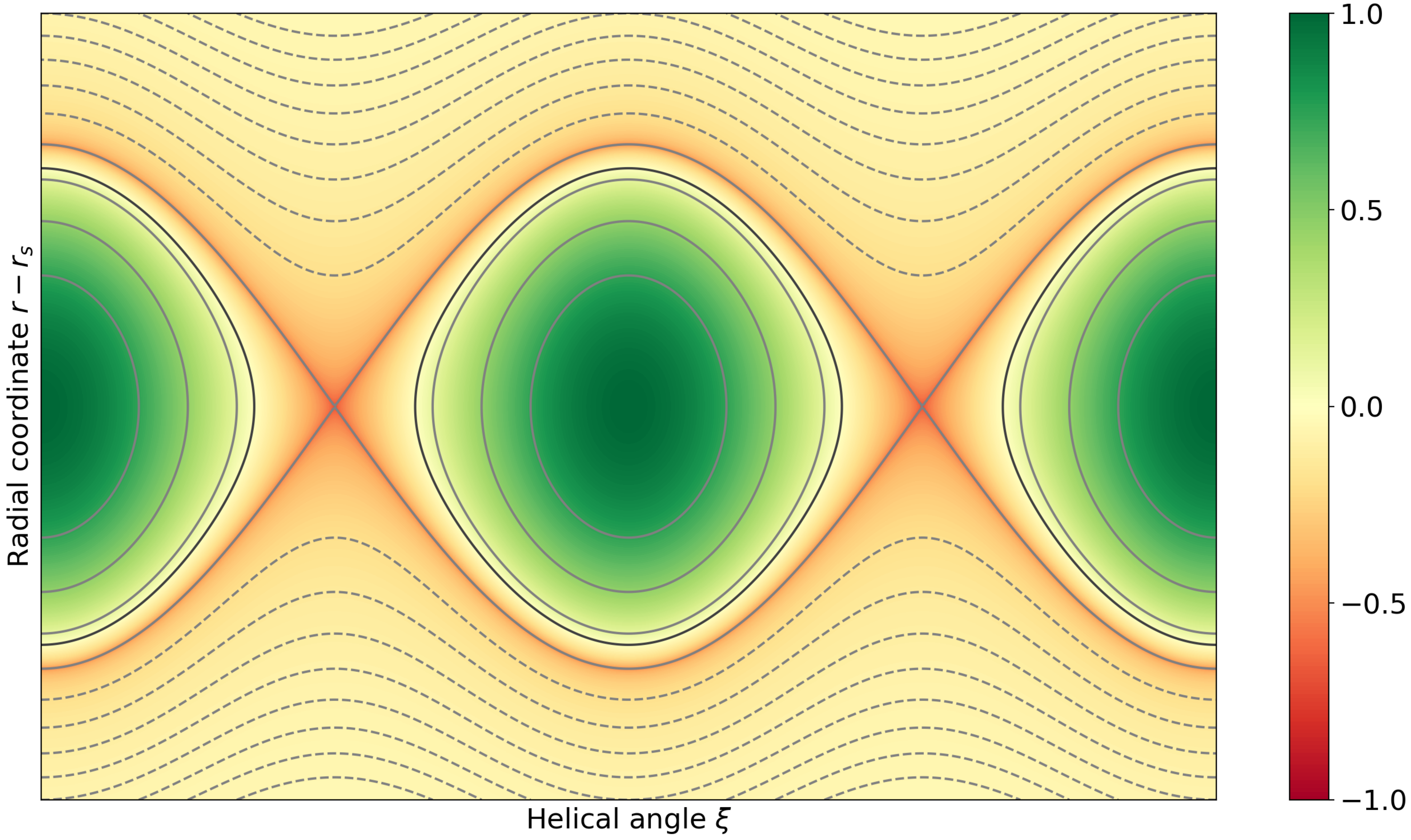

Island radial width largest at O-point

$\Rightarrow \eta_{\mathrm{stab}}$ for LM stabilization is higher and less sensitive to broadening, misalignment

[2] Brookman et al. 2021
[3] Snicker et al. 2018

The case for Locked Mode stabilization

In large devices, in particular ITER…

… Rotating island stabilization is challenging, may not be viable

Fast mode locking + RF broadening

… Locked modes do not have to be avoided at all cost

Small w_{lock} and large $\tau_M \Rightarrow$ no immediate disruption or loss of H-mode

… It is preferable to stabilize locked instead of rotating modes

Higher η_{stab} & small $w_{\text{lock}} \Rightarrow$ lower peak RF power

Not limited by fast locking or large $w_{\text{seed}} \Rightarrow$ more robust

RF power does not need to be always on $\Rightarrow$ lower average RF power

Perceived reasons to avoid LMs

… *"⇒ disruption"*: small $w_{\mathrm{lock}}/a \lesssim 5\,\%$ far from $w_{\mathrm{disr}}/a \sim 30\,\%$ [4]

… *"locking to error field ⇒ inaccessible to ECCD"*:

Use static external fields to lock island in front of ECCD, as demonstrated on DIII-D [5].

In ITER: passively adjust already present error field correction coils, not necessarily higher EF.

… *"loss of rotation (and H-mode)"*: yes and no,

- time window $\sim \tau_M$ between locking and loss of H-mode [6].
  H-mode preserved if fast stabilization after locking, even for large DIII-D island [5,7].

[4] de Vries et al. 2016
[5] Volpe et al. 2015
[6] Nelson et al. 2020
[7] Volpe 2017

Perceived reasons to avoid LMs

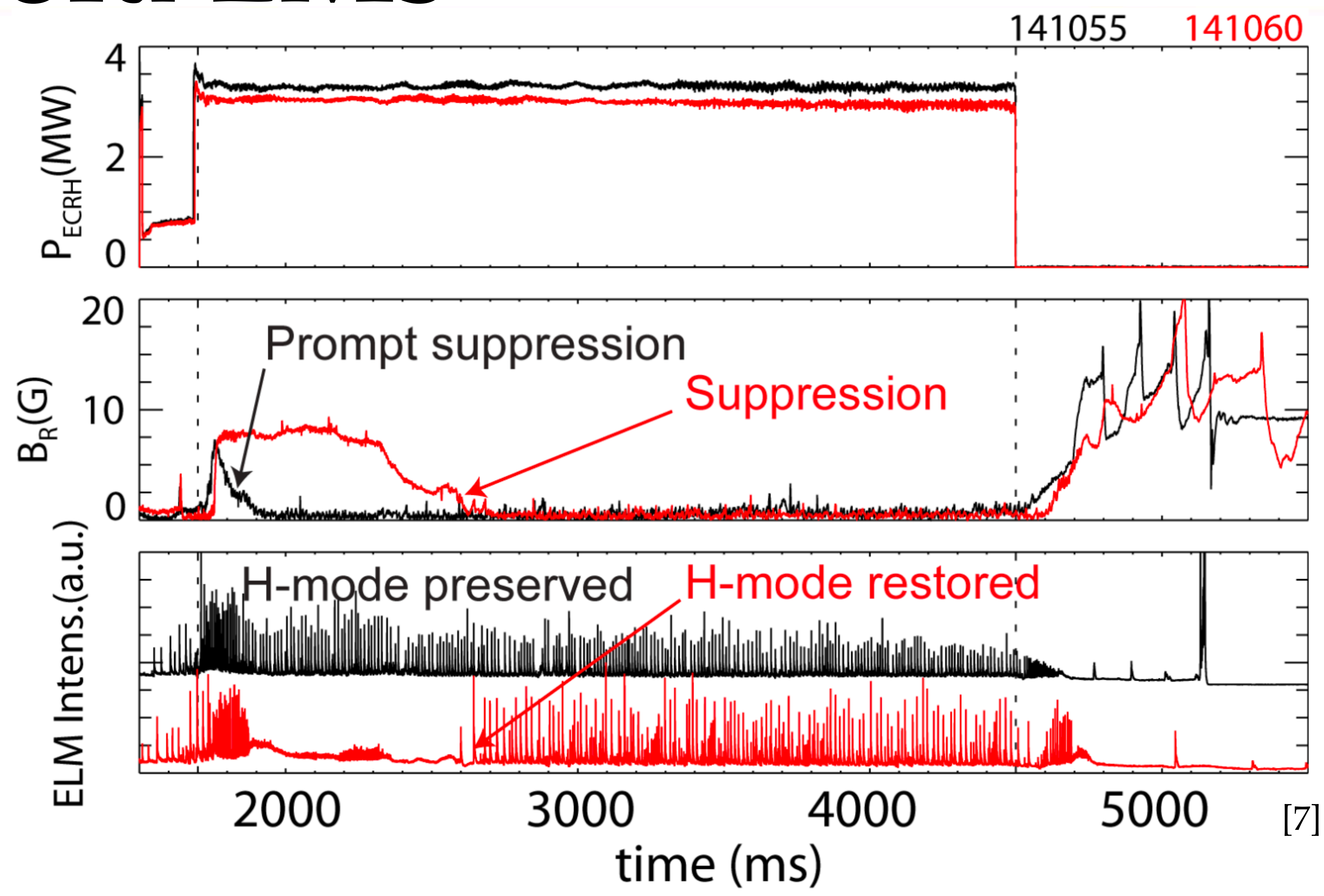

… *"loss of rotation (and H-mode)"*: yes and no,

- time window ~ τ_M between locking and loss of H-mode [6].
H-mode preserved if fast stabilization after locking, even for large DIII-D island [5,7].

- for small w_{lock}, small impact on confinement, like small island at pedestal top during RMP ELM-suppression experiments? [8]

[5] Volpe et al. 2015
[6] Nelson et al. 2020
[7] Volpe 2017
[8] Evans et al. 2004

The case for Locked Mode stabilization

Hard to avoid LMs in large tokamaks like ITER…

… but small LMs are tolerable …

⇒ Prepare LM Stabilization strategy, at least as back-up.

Can even consider stabilization of large LMs to further reduce disruptivity: see A. Reiman talk Friday 11:10

… It might be preferable to stabilize locked instead of rotating modes

Higher η_{stab} & small w_{lock} ⇒ lower peak RF power

Not limited by fast locking or large w_{seed} ⇒ more robust

RF power does not need to be always on ⇒ lower average RF power

Island evolution

Generalized Rutherford Equation

$$0.82\frac{\tau_r}{r_s}\frac{\mathrm{d}w}{\mathrm{d}t} = \underbrace{r_s\left[\Delta_0' - \Delta_{0,\mathrm{wall}}'(\omega)\right]}_{\text{Classical [1,9]}} + \underbrace{2m\left(\frac{w_{\mathrm{vac}}}{w}\right)^2\cos(\phi-\phi_{\mathrm{EF}})}_{\text{Error field / RMP [10]}} + a_2\frac{j_{\mathrm{BS}}}{j_{\|}}L_q\left(\underbrace{\frac{2}{3w}-\frac{3w_{\mathrm{ib}}^2}{w^3}}_{\substack{\text{Bootstrap and}\\ \text{polarisation [1]}}} - \underbrace{\frac{3\pi^{3/2}}{4w_{\mathrm{dep}}}\frac{w_{\mathrm{dep}}^2}{w^2}\eta_{\mathrm{NTM}}\eta_{\mathrm{aux}}}_{\text{Current drive [11]}}\right)$$

Torque Equation

$$\frac{\mathrm{d}\omega}{\mathrm{d}t} = \underbrace{\frac{\omega_0(\tau_M/\tau_{M0})-\omega}{\tau_M}}_{\text{Viscous [1]}} - \frac{1}{\tau_{A0}^2}\left(\frac{w}{a}\right)^3\left[\underbrace{\frac{C_1}{m}\frac{\omega\tau_w}{(\omega\tau_w)^2+1}}_{\text{Resistive wall [1,9]}} + \underbrace{\frac{m^2}{256}\left(\frac{a}{L_q}\right)^2\left(\frac{w_{\mathrm{vac}}}{w}\right)^2\sin(\phi-\phi_{\mathrm{EF}})}_{\text{Error field / RMP [10]}}\right]$$

and $\dot{\phi}=\omega$ to resolve ϕ dependencies of EF terms and η_{aux}.

Extension of previous work in [2,10,11]. More details on each term in Appendix.

[1] La Haye et al. 2017
[9] Nave & Wesson 1990
[10] Fitzpatrick 1993
[11] De Lazzari & Westerhof 2009
[12] van den Brand et al. 2012
[13] La Haye et al. 2006

Locked 2/1 NTM stabilization in ITER

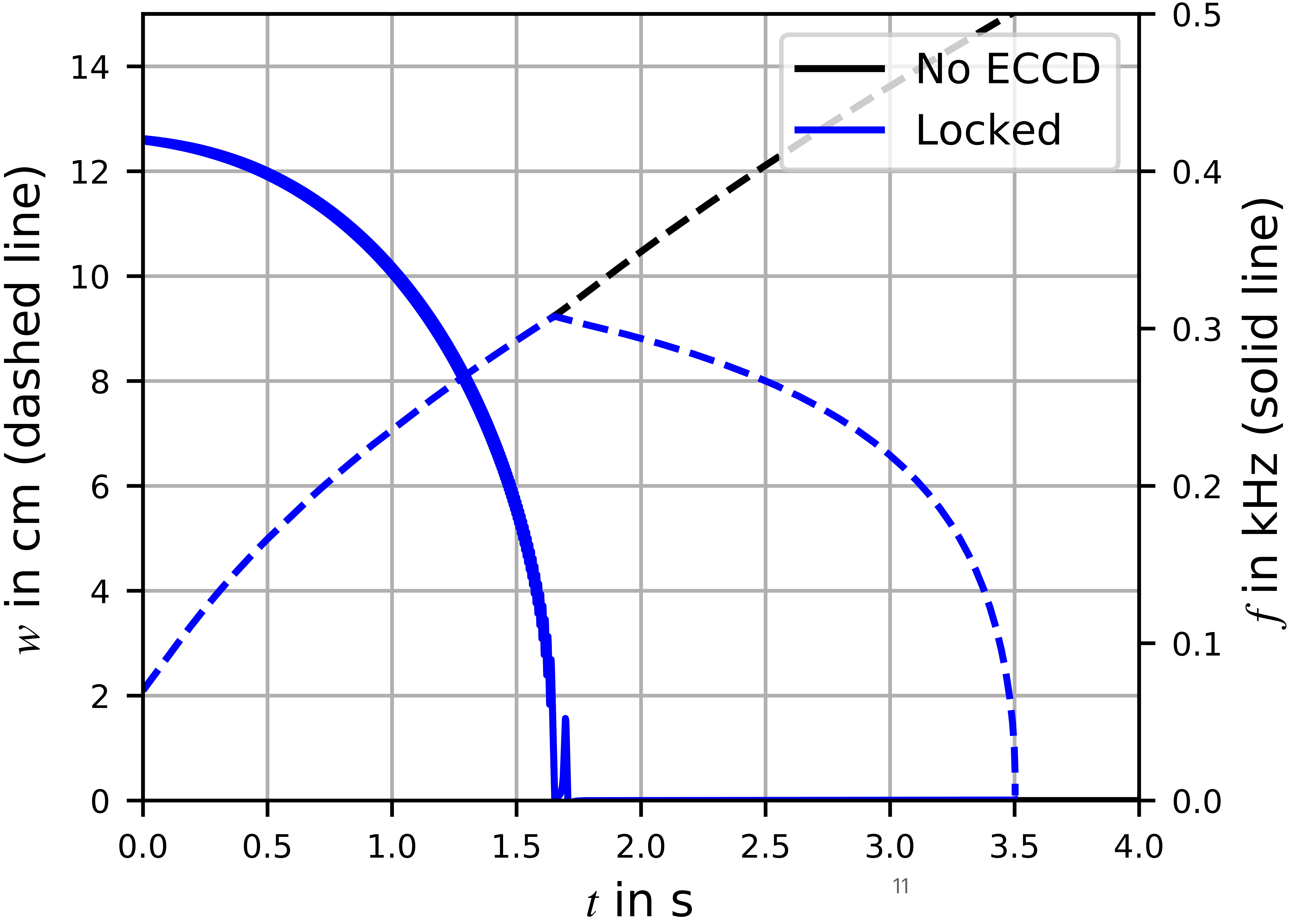

Base settings:
$w_{\text{seed}} = 2.1$ cm
$w_{\text{vac}} = 2.5$ cm

EC settings:
η_{CD} for LSM, $\beta = 20°$ [14]
$P_{\text{EC}} = 7.5$ MW
Broadening factor 3
$x_{\text{mis}} = 0$ cm

Locked Mode can be quickly stabilized with moderate P_{EC}, even for large broadening

[14] Bertelli et al. 2011

Peak power: broadening

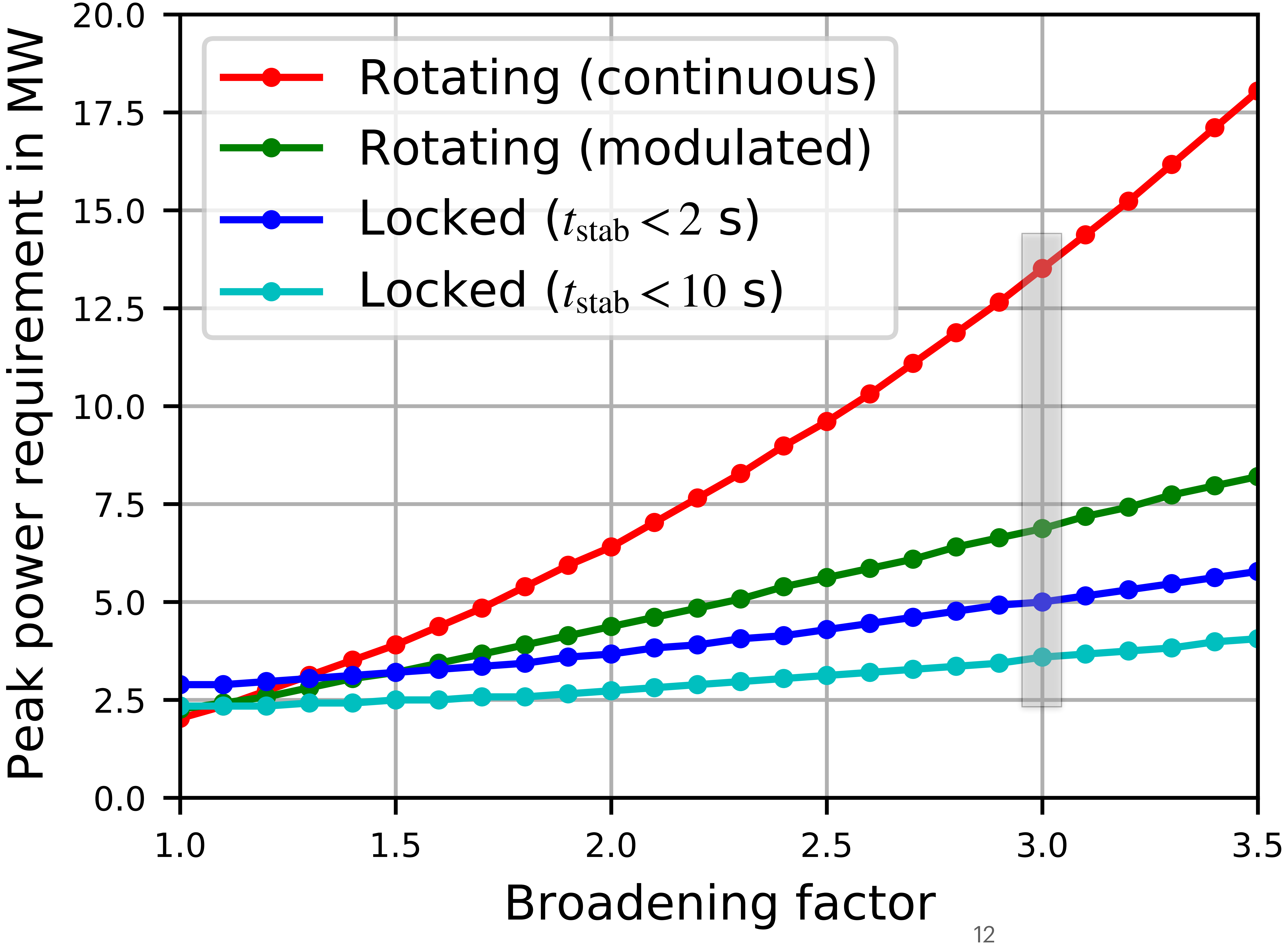

Base settings:
$w_{seed} = 2.1$ cm
$w_{vac} = 2.5$ cm
$w_{detect} = 4$ cm

For broadening factors $\gtrsim 1.5$, Peak power requirement is lowest for locked mode stabilization

Peak power: seeding width

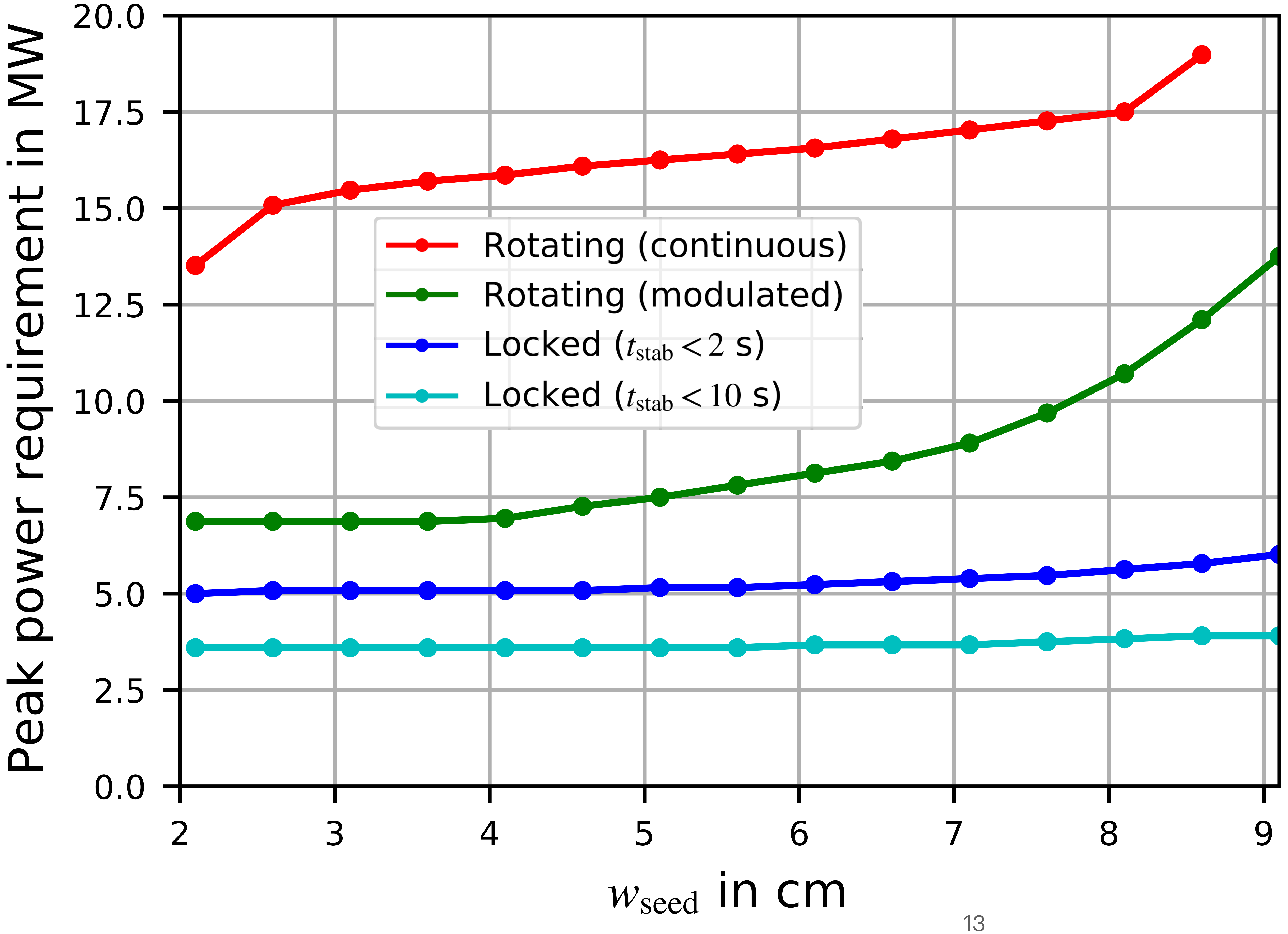

Base settings:
Broadening = 3
$w_{\text{vac}} = 2.5$ cm
$w_{\text{detect}} = 4$ cm

Locked mode stabilization is more robust to large seeding events

Average power lowest for locked mode stab.

Rotating (continuous):
if preemptive stabilization,
power always on, $P_{\text{avg}} = P_{\text{peak}}$

Rotating (modulated):
Without CD, $\dot{w} > 0$ for $w > w_{\text{marg}}$
so if $w_{\text{detect}} \sim 4$ cm $> w_{\text{marg}} \sim 1.5$ cm [1],
power always on, $P_{\text{avg}} = P_{\text{peak}}$.

(if $w_{\text{detect}} > w_{\text{crit}} \sim 4.5$ cm [1],
can't even prevent locking!)

Locked mode:
power on only during stabilization,

$$P_{\text{avg}} = P_{\text{peak}} \frac{t_{\text{stab}}}{t_{\text{stab}} + t_{\text{seed}} + t_{\text{lock}}}$$

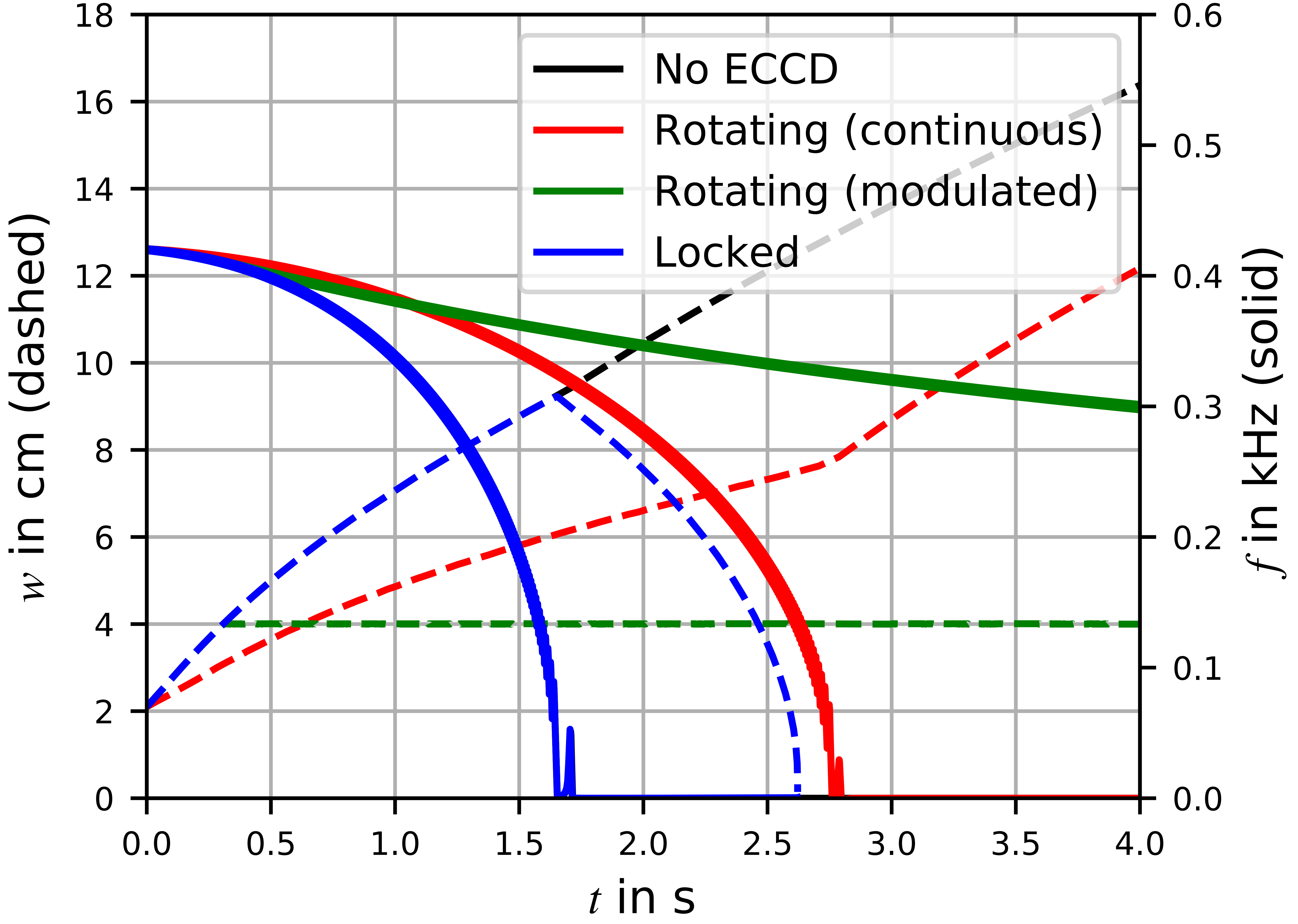

[1] La Haye et al. 2017

The case for Locked Mode stabilization

Hard to avoid LMs in large tokamaks like ITER…

… but small LMs are tolerable …

⇒ Prepare LM Stabilization strategy, at least as back-up.

Can even consider stabilization of large LMs to further reduce disruptivity: see A. Reiman talk Friday 11:10

Can stabilize small LM with low peak and average EC power,…

… more robust to broadening, misalignment and large seeding.

⇒ No need to stabilize rotating mode, let island lock.

Large potential impact on ITER fusion gain and disruptivity, need to pay more attention to Locked Modes.

https://arxiv.org/abs/2106.06581

Thank you!

Questions and feedback are welcome

https://arxiv.org/abs/2106.06581

References

[1] La Haye, R. J., Paz-Soldan, C. & Liu, Y. Q. Effect of thick blanket modules on neoclassical tearing mode locking in ITER. *Nucl. Fusion* **57**, 014004 (2017).

[2] Polevoi, La Haye, *private comm.* (2019)

[2$^{3/4}$] Brookman, M. W. *et al.* Resolving ECRH Deposition Broadening Due to Edge Turbulence in DIII-D. *Physics of Plasmas* **28**, (2021)

[3] Snicker, A. *et al.* The effect of density fluctuations on electron cyclotron beam broadening and implications for ITER. *Nucl. Fusion* **58**, 016002 (2018).

[4] Vries, P. C. *et al.* The Influence of an ITER-like Wall on Disruptions at JET. *Physics of Plasmas* **21** (2014).

[5] Volpe, F. A. *et al.* Avoiding Tokamak Disruptions by Applying Static Magnetic Fields That Align Locked Modes with Stabilizing Wave-Driven Currents. *Physical Review Letters* **115**, (2015).

[6] Nelson, A.O. *et al.* Experimental evidence of ECCD-based NTM suppression threshold reduction during mode locking on DIII-D. *Plasma Phys. Control. Fusion* **in press,** (2020)

[7] F. Volpe, presentation at Madison MHD control workshop (2017), https://pl.apam.columbia.edu/files/seaspllab/presentations/2017_MHDWS_volpe_LMReview.pdf

[8] Evans, T. E. *et al.* Suppression of Large Edge-Localized Modes in High-Confinement DIII-D Plasmas with a Stochastic Magnetic Boundary. *Physical Review Letters* **92**, (2004).

[9] Nave, M. F. F. & Wesson, J. A. Mode locking in tokamaks. *Nucl. Fusion* **30**, 2575–2583 (1990).

[10] Fitzpatrick, R. Interaction of tearing modes with external structures in cylindrical geometry (plasma). *Nucl. Fusion* **33**, 1049–1084 (1993).

[11] De Lazzari, D. & Westerhof, E. On the merits of heating and current drive for tearing mode stabilization. *Nuclear Fusion* **49**, 075002 (2009).

[12] van den Brand, H., de Baar, M. R., Cardozo, N. J. L. & Westerhof, E. Integrated modelling of island growth, stabilization and mode locking: consequences for NTM control on ITER. *Plasma Phys. Control. Fusion* **54**, 094003 (2012).

[13] Haye, R. J. L. *et al.* Cross–machine benchmarking for ITER of neoclassical tearing mode stabilization by electron cyclotron current drive. *Nucl. Fusion* **46**, 451–461 (2006).

[14] Bertelli, N. e*t al*. Requirements on Localized Current Drive for the Suppression of Neoclassical Tearing Modes. *Nuclear Fusion* **51** (2011).

[15] Yu, Q. & Günter, S. Locking of neoclassical tearing modes by error fields and its stabilization by RF current. *Nucl. Fusion* **48**, 065004 (2008).

[16] Hender, T. C. *et al.* Chapter 3: MHD stability, operational limits and disruptions. *Nucl. Fusion* **47**, S128–S202 (2007).

[17] Glasser, A. H., Greene, J. M. & Johnson, J. L. Resistive instabilities in general toroidal plasma configurations. *The Physics of Fluids* **18**, 875–888 (1975).

[18] Fitzpatrick, R. Helical temperature perturbations associated with tearing modes in tokamak plasmas. *Physics of Plasmas* **2**, 825–838 (1995).

Appendix 1:

Glossary of quantities and values

Values used in simulations (mostly from [1])

Resistive time: $\tau_R = \mu_0 r_s^2 \eta^{-1}$

Radius of $q = 2$ surface: $r_s = 155$ cm

Resistivity: $\eta^{-1} = 1258(T_e/1\text{ eV})^{3/2} f_\epsilon / Z_{\text{eff}}$

Electron temperature: $T_e = 5.63$ keV

Trapped particle fraction: $f_\epsilon = 0.26$

Effective ion charge [2]: $Z_{\text{eff}} = 1.53$

Shear length: $L_q = 94$ cm

Bootstrap current: $j_{\text{BS}} = 7.2 \cdot 10^4$ A/m^2

Average parallel current:
$j_{\|} = 38.8 \cdot 10^4$ A/m^2

Radius of resistive wall: $r_w = 1.25\, a$

Resistive wall time: $\tau_w = 14$ ms

Alfven time: $\tau_{A0} = 3\ \mu$s

Original rotation frequency:
$\omega_0 = 2\pi \cdot 0.42$ kHz

Original momentum confinement time:
$\tau_{M0} = 3.7$ s

Fitting coefficients: $C_1 = 1/80, \quad C_M = 12$

[1] La Haye et al 2017
[2] Polevoi & La Haye 2019

Appendix 2:

Rutherford equation term by term

Classical tearing index Δ_0'

The classical tearing mode contribution is given by the jump in the derivative of the magnetic perturbation ψ at the rational surface r_s:

$$r_s \Delta_0' = \frac{\frac{\partial \psi}{\partial r}(r_s^+) - \frac{\partial \psi}{\partial r}(r_s^-)}{\psi(r_s)}.$$

For a fast rotating island, the resistive wall acts like a perfect conductor, thus giving an additional stabilizing contribution which can be approximated as [9]

$$r_s \Delta_{\mathrm{wall}}' = -2m \left(\frac{r_s^+}{r_w}\right)^{2m} \frac{(\omega\tau_w)^2 \left[1 - \left(\frac{r_s^+}{r_w}\right)^{2m}\right]}{1 + (\omega\tau_w)^2 \left[1 - \left(\frac{r_s^+}{r_w}\right)^{2m}\right]^2},$$

where r_w is the wall radius, τ_w the resistive wall time and ω the island rotation frequency.

[9] Nave & Wesson 1990

Error field or RMP $\Delta'_{\mathrm{EF,RMP}}$

The error field or RMP term is given by [10]

$$r_s \Delta'_{\mathrm{EF,RMP}} = 2m \left(\frac{w_{\mathrm{vac}}}{w} \right)^2 \cos(\phi - \phi_{\mathrm{EF}}),$$

The vacuum island width is obtained from the magnetic field perturbation at the edge [10], which can be related to the radial error field at the plasma edge $b_{\mathrm{rn}} = B_r/B_t = m\psi(a)a$ [16], such that

$$w_{\mathrm{vac}} = 4a \sqrt{b_{\mathrm{rn}} \frac{B_t}{mB_p} \frac{L_q}{a} \left(\frac{r_s}{a} \right)^m} = \sqrt{\frac{b_{\mathrm{rn}}}{10^{-5}}} \cdot 2.2 \text{ cm}$$

To avoid error field penetration, ITER has a 3-field requirement

$$B_{3-\mathrm{mode}} = \sqrt{B_{2,1}^2 + 0.8 B_{3,1}^2 + 0.2 B_{r1,1}^2} \leq 5 \cdot 10^{-5} B_t \,.$$

It thus makes sense to take $w_{\mathrm{vac}} \sim 2.5 - 5.0$ cm.

[10] Fitzpatrick 1993
[16] Hender et al. 2007

Bootstrap current Δ'_{BS}

The bootstrap term is modeled as [1, 13]

$$r_s \Delta'_{\mathrm{BS}} = \left(a_2 \frac{j_{\mathrm{BS}}}{j_{\|}} L_q \right) \frac{2}{3w},$$

where $a_2 = 2.8$ is a parameter fitted from experiment [13] to include toroidal effects in the bootstrap term, whereas $a = 4$ for a cylinder, so toroidal effects slightly reduce the magnitude of the bootstrap term. Furthermore, the factor 2/3 originates from an additional stabilising Glasser-Greene-Johnson [17] contribution, obtained by experimental fit [1].

Note that, for consistency with [1, 13], no incomplete pressure flattening term was included here, which would modify the bootstrap term at small island width as [18]

$$\frac{1}{w} \to \frac{w}{w^2 + w_{\mathrm{tra}}^2}.$$

[1] La Haye et al. 2017
[13] La Haye et al. 2013
[17] Glasser et al. 1975
[18] Fitzpatrick 1995

Polarization current Δ'_{pol}

The polarization current is modeled as [1]

$$r_s \Delta'_{\text{pol}} = -\left(a_2 \frac{j_{\text{BS}}}{j_{\|}} L_q \right) \frac{3 w_{\text{ib}}^2}{w^3},$$

with the ion banana width $w_{\text{ib}} \sim \epsilon^{1/2} \rho_{\theta,i} \approx 0.7$ cm.

The term stabilizes the island at small widths. The combination of bootstrap and polarisation current terms is negative (stabilizing) for $w < 3w_{\text{ib}}/\sqrt{2} \sim 2.1 w_{\text{ib}}$ and maximal for $w = \sqrt{3/2} \cdot 3w_{\text{ib}} \sim 3.7 w_{\text{ib}}$.

[1] La Haye et al. 2017

Current drive Δ'_{CD}

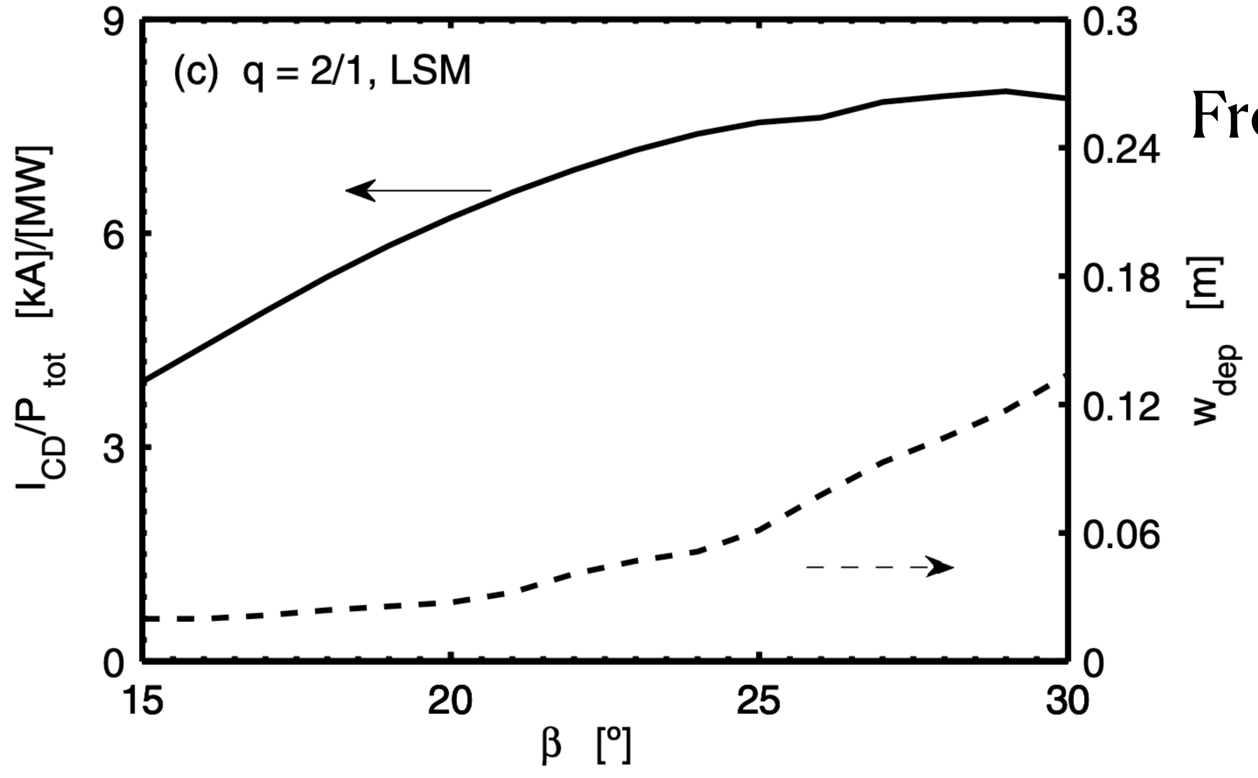

From [14]

The current drive term is modeled as [11]

$$r_s\Delta'_{\mathrm{CD}} = -\left(a_2\frac{j_{\mathrm{BS}}}{j_{\|}}L_q\right)\frac{3\pi^{3/2}}{4w_{\mathrm{dep}}}\frac{w_{\mathrm{dep}}^2}{w^2}\eta_{\mathrm{NTM}}\eta_{\mathrm{aux}},$$

where w_{dep} is the $1/e$ width of the gaussian deposition and $\eta_{\mathrm{NTM}} = j_{\mathrm{CD,max}}/j_{\mathrm{BS}}$. The peak driven current $j_{\mathrm{CD,max}} = P_{\mathrm{tot}}\gamma_{\mathrm{CD}}$, with the quantity $\gamma_{\mathrm{CD}} = j_{\mathrm{CD,max}}/P_{\mathrm{tot}} \propto (I_{\mathrm{CD}}/w_{\mathrm{dep}})/P_{\mathrm{tot}}$ a measure of the current drive efficiency. The quantity $I_{\mathrm{CD}}/P_{\mathrm{tot}}$ is approximately constant for a given toroidal launching angle. We thus take γ_{CD} to match the value in [14] and appropriately decrease the peak current density when including broadening effects. Broadening leaves P_{tot} unchanged, but reduces $j_{\mathrm{CD,max}}$, so γ_{CD}must also be reduced accordingly.

The stabilization efficiency is given by [11]

$$\eta_{\mathrm{aux}} = \frac{\int_{-1}^{\infty}\mathrm{d}\Omega\,\langle p_{\mathrm{EC}}\rangle\frac{\langle\cos(m\xi)\rangle}{\langle 1\rangle}}{\int_{-1}^{\infty}\mathrm{d}\Omega\,\langle p_{\mathrm{EC}}\rangle},$$

where $\Omega = 8x^2/w^2 - \cos(m\xi)$ is a flux coordinate ($\Omega = -1$ at the island O-point and $\Omega = 1$ at the separatrix), $\xi = \theta - n/m\phi$ a helical angle and angular brackets indicate flux surface averages. The power deposition is assumed to be a gaussian in the radial direction and a delta function in the helical angle,

$$p_{\mathrm{EC}} \propto \exp\left(-4(x - x_{\mathrm{dep}})^2/w_{\mathrm{dep}}^2\right)\delta(m\xi - \phi + \phi_{\mathrm{EC}}).$$

The stabilization efficiency is evaluated instantaneously as the phase evolves, even for the rotating island. Note in particular that no fast rotation needs to be assumed for the rotating island case, and that no arithmetic approximations to the stabilization efficiency are used.

[11] De Lazzari & Westerhof 2009
[14] Bertelli et al. 2011

Appendix 3:

Equation of angular motion term by term

Viscous torque T_{visc}

The viscous torque is modeled as [1]

$$\dot{\omega}_{\text{visc}} = \frac{\omega_0(\tau_M/\tau_{M0}) - \omega}{\tau_M},$$

where $\tau_{M0} = 3.7$ s is the momentum confinement time without island, and $\tau_M = \tau_{M0}/(1 + C_M w/a)$ takes into account the confinement degradation due to the island's presence, with $C_M = 12$ fitted to a DIII-D Iter Baseline Scenario (IBS) shot [1]. The original rotation frequency $\omega_0 = 2\pi f_0$, with $f_0 = 0.42$ kHz.

The viscous torque tries to restore the island rotation to the background plasma rotation.

[1] La Haye et al. 2017

Resistive wall torque T_{wall}

The resistive wall torque is modeled as [1,9]

$$\dot{\omega}_{\text{wall}} = -\frac{1}{\tau_{A0}^2}\left(\frac{w}{a}\right)^3 \frac{C_1}{m}\frac{\omega\tau_w}{(\omega\tau_w)^2+1},$$

where $\tau_{A0} = 3.0\ \mu$s is an Alfven time, $\tau_w = 14$ ms is the wall time of ITER's blanket and $C_1 = 1/80$ [1] (note there was a mistake in the original paper incorrectly reporting $C_1 = 1/20$).

Note the w^3 dependence instead of the w^4 dependence in [9], which originates from taking the island inertia instead of that of the entire plasma, see [1,13].

The resistive wall torque is the main reason for the fast braking of the island. The balance with the viscous torque gives the critical island width, $w_{\text{crit}} \sim 4$ cm in ITER, above which there is no fast rotating steady-state solution to the equation of angular motion, i.e. the island is on course for locking.

[1] La Haye et al. 2017
[9] Nave & Wesson 1990
[13] La Haye et al. 2012

Error field/RMP torque $T_{\mathrm{EF,RMP}}$

The error field torque is modeled as [10]

$$\dot{\omega}_{\mathrm{EF/RMP}} = -\frac{1}{\tau_{A0}^2}\left(\frac{w}{a}\right)^3 \frac{m^2}{256}\left(\frac{a}{L_q}\right)^2 \left(\frac{w_{\mathrm{vac}}}{w}\right)^2 \sin(\phi - \phi_{\mathrm{EF}}),$$

where the original formula from [10] was modified to use the island inertia instead of that of the entire plasma (see previous page and [1,13]).

If the rotation frequency is seen as a ball, the error field torque is like a hill. Once the ball is trapped in the hill, it is generally quickly decelerated and finally trapped at a phase close to the error field phase (depending on the relative strength of error field and viscous torques).

[1] La Haye et al. 2017
[10] Fitzpatrick 1993
[13] La Haye et al. 2012

Example evolution without ECCD

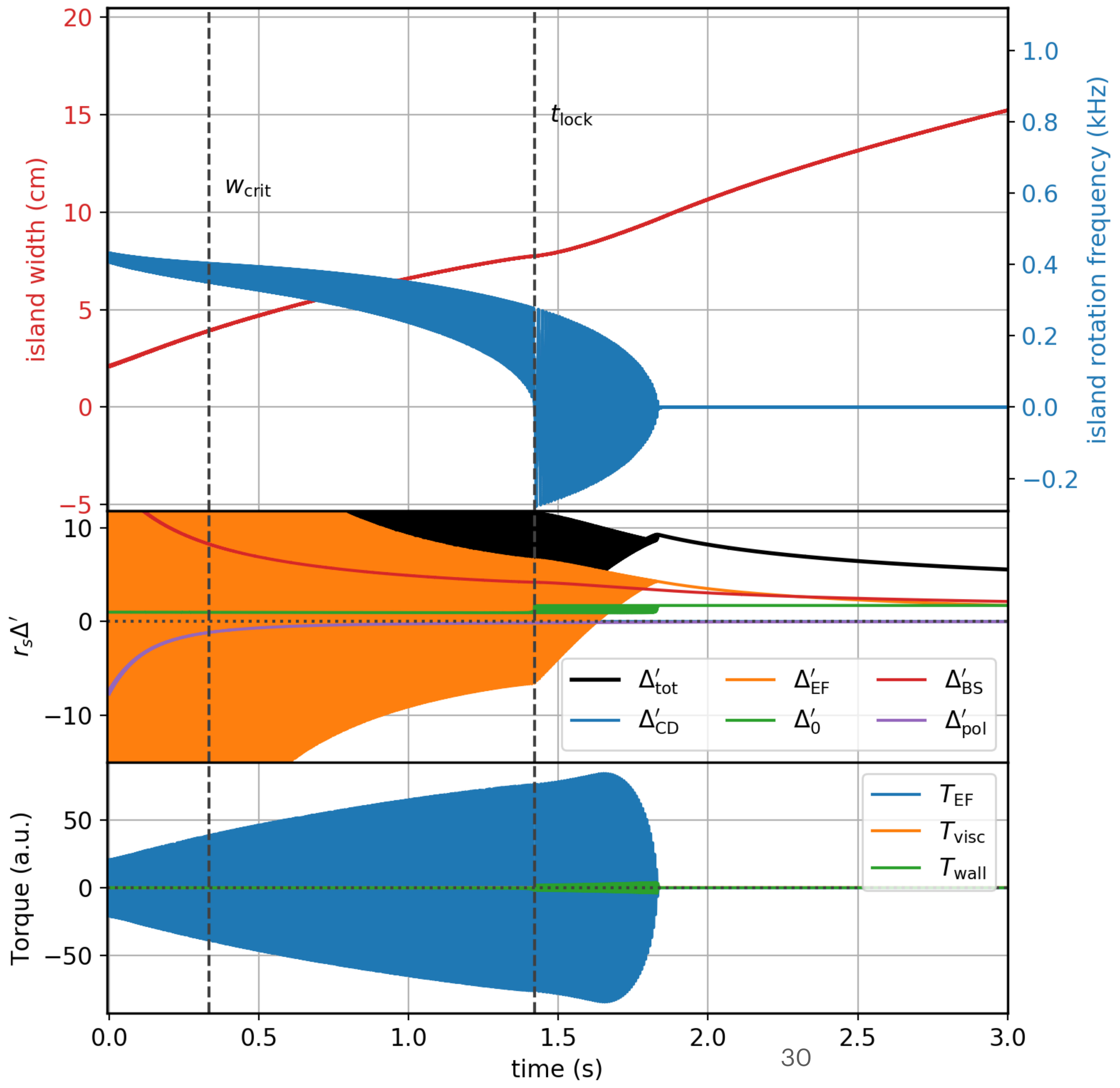

here, large $w_{\mathrm{vac}} = 10$ cm, $(B_{\mathrm{r}}(a) \sim 2 \cdot 10^{-4} B_\phi \sim 10\ \mathrm{G})$

locking at $\phi \approx \phi_{\mathrm{EF}}$

driven reconnection after locking

Appendix 4:

Optimal toroidal launching angle, different scenarios, detection threshold, error field, …

(Older plots that used slightly different parameters, Results should still hold qualitatively)

Optimal toroidal launching angle

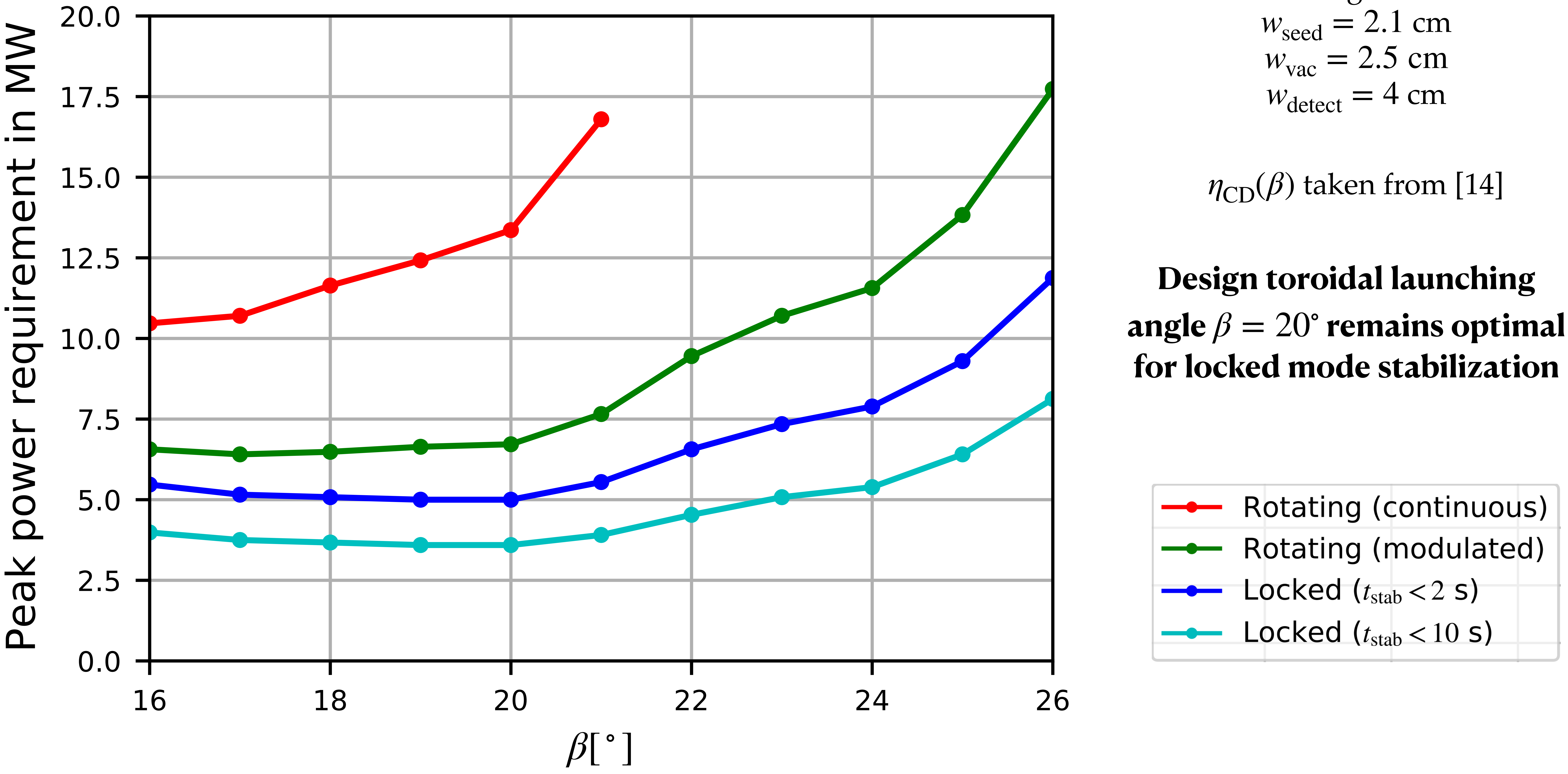

Base settings:
Broadening factor of 3
$w_{seed} = 2.1$ cm
$w_{vac} = 2.5$ cm
$w_{detect} = 4$ cm

$\eta_{CD}(\beta)$ taken from [14]

Design toroidal launching angle $\beta = 20^\circ$ remains optimal for locked mode stabilization

[14] Bertelli et al. 2011

Power requirement with combined stabilization

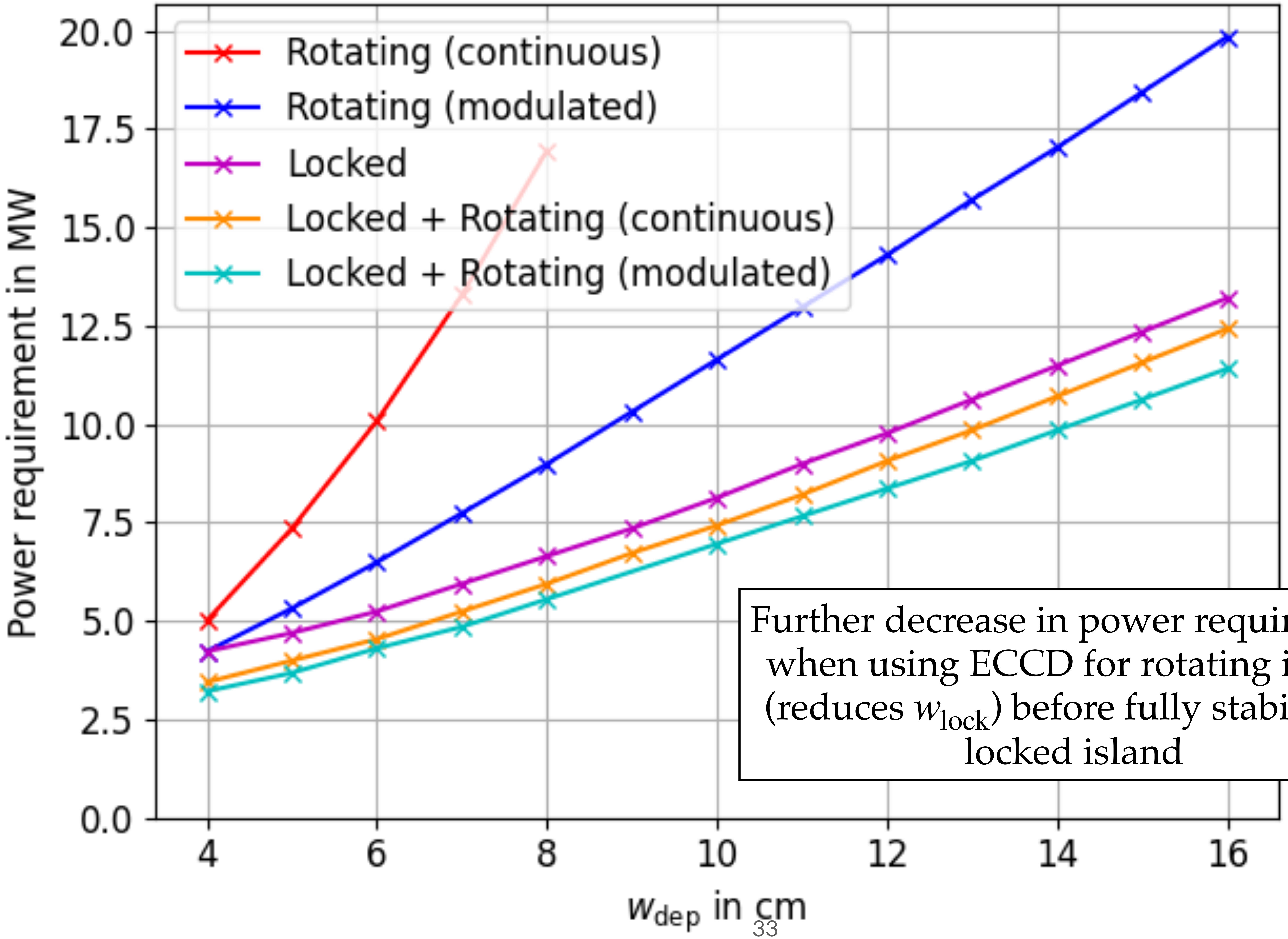

$w_{vac} = 2.5$ cm
$w_{dep} = 8$ cm
$x_{mis} = 1$ cm

Further decrease in power requirement when using ECCD for rotating island (reduces w_{lock}) before fully stabilizing locked island

Time delay / detection threshold

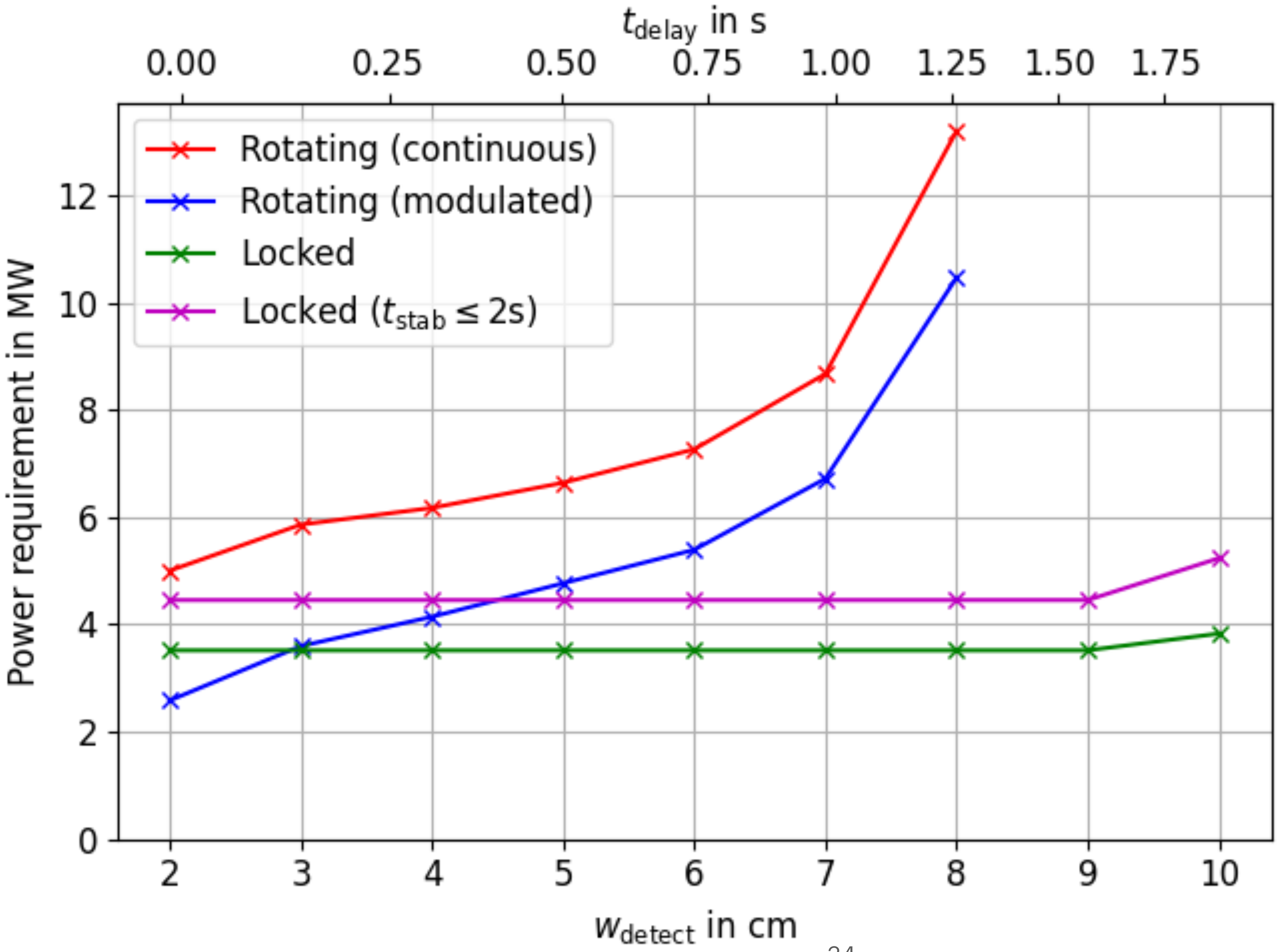

ECCD is turned on when $w > w_{\text{detect}}$, or $t - t_{\text{seed}} > t_{\text{delay}}$.

The two can be combined, e.g. $w_{\text{detect}} = 4$ cm $\Leftrightarrow t_{\text{delay,det}} = 0.3$ s and actual $t_{\text{delay,act}} = 0.5$ s. Then, in plot, $t_{\text{delay}} = 0.8$ s $\Leftrightarrow w_{\text{detect}} = 6.25$ cm

Radial misalignment

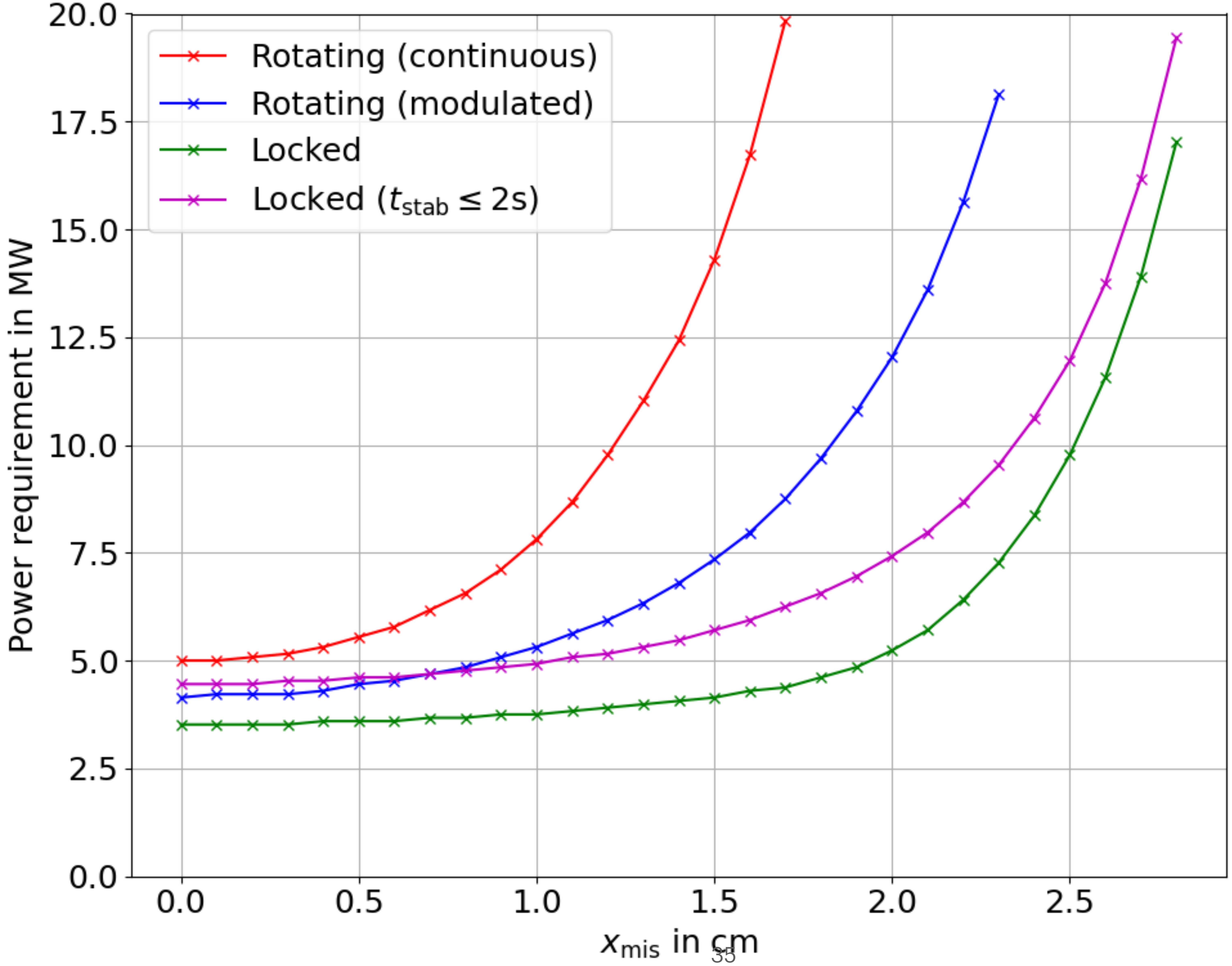

$w_{vac} = 2.5$ cm
$w_{seed} = 2.1$ cm
$w_{dep} = 4$ cm

Error field: power requirement and spin-up

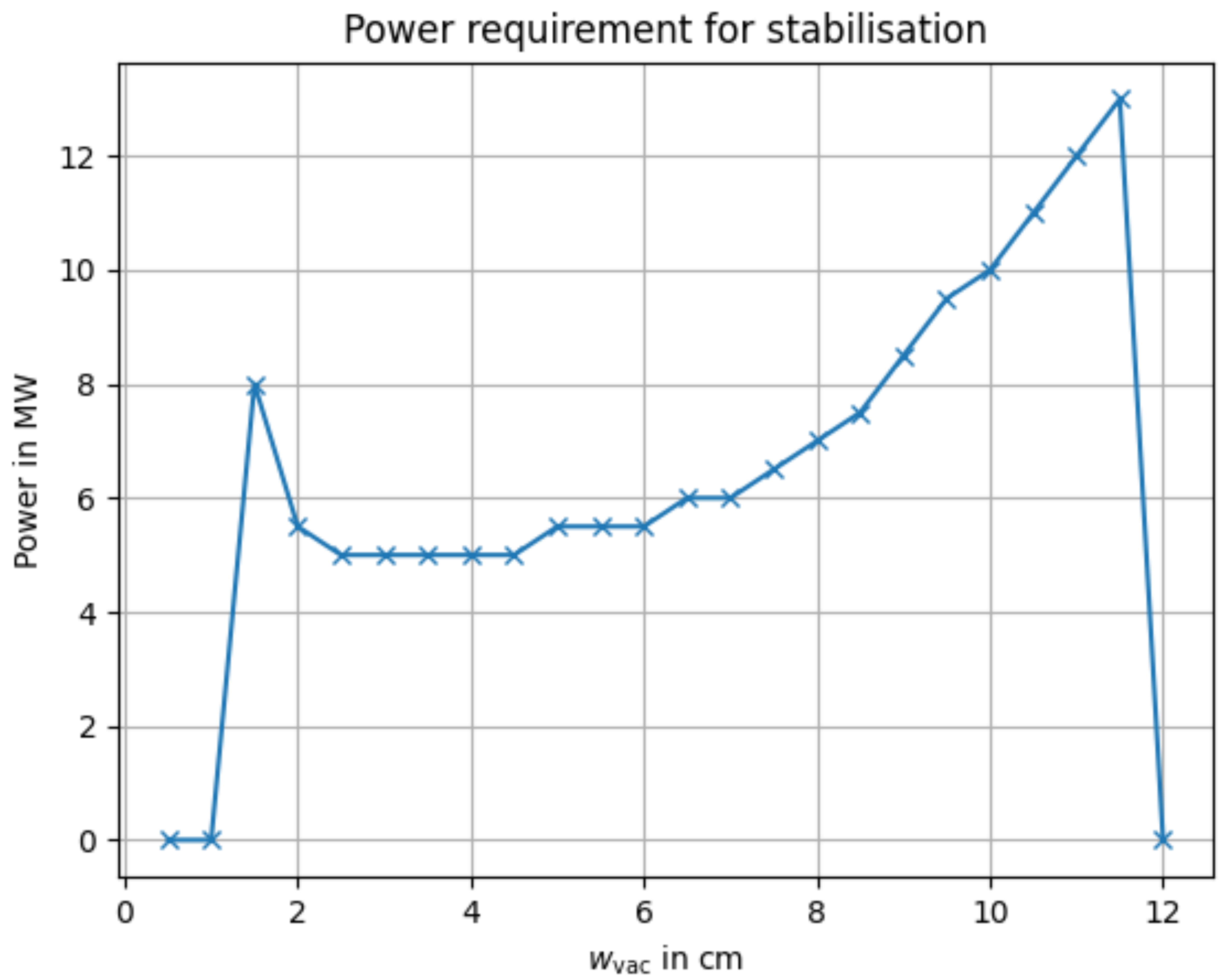

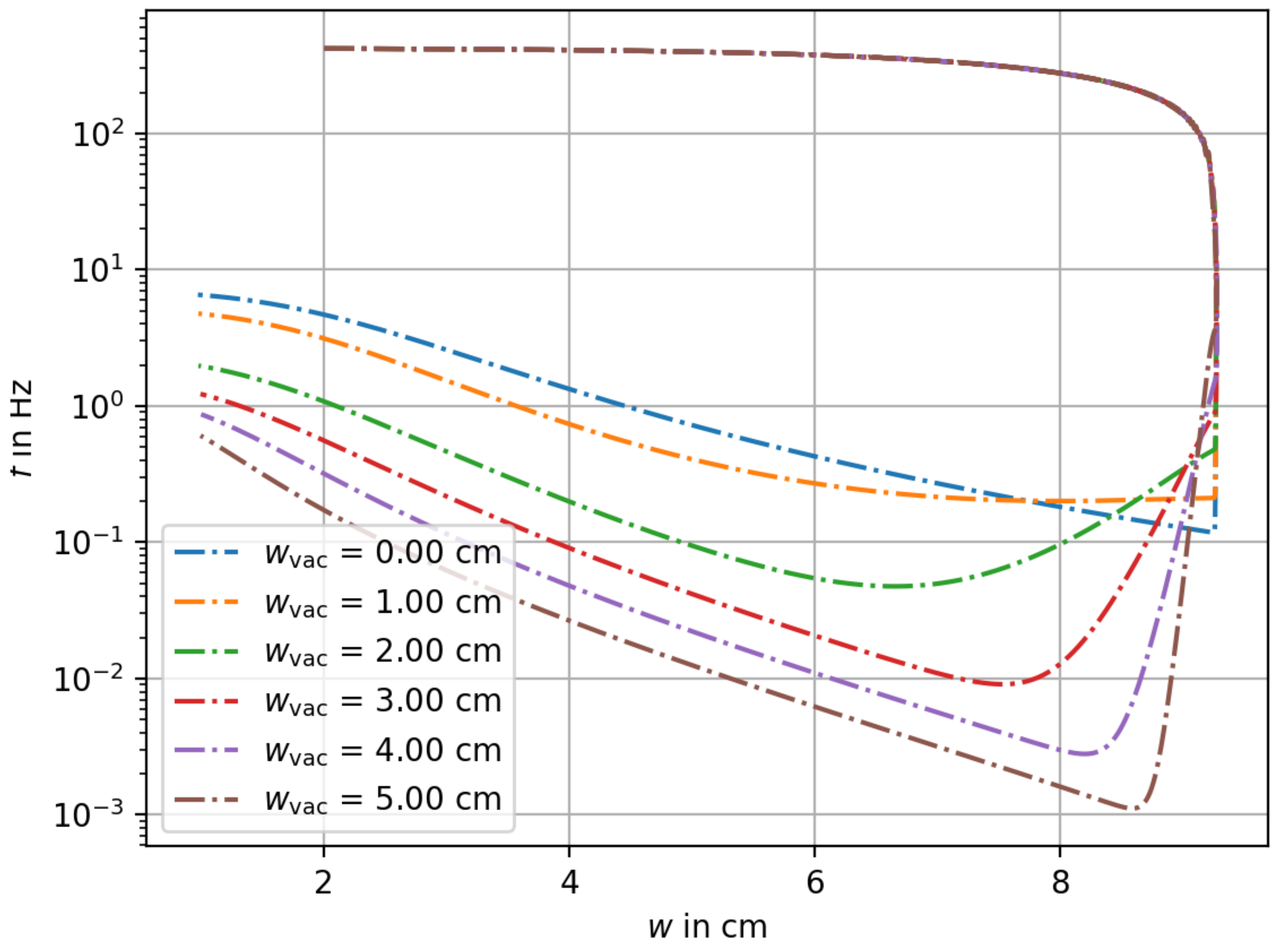

Appendix 5:

Geometry of NTM stabilization

Geometry of NTM stabilization

Plot of local stabilization efficiency η_{aux}

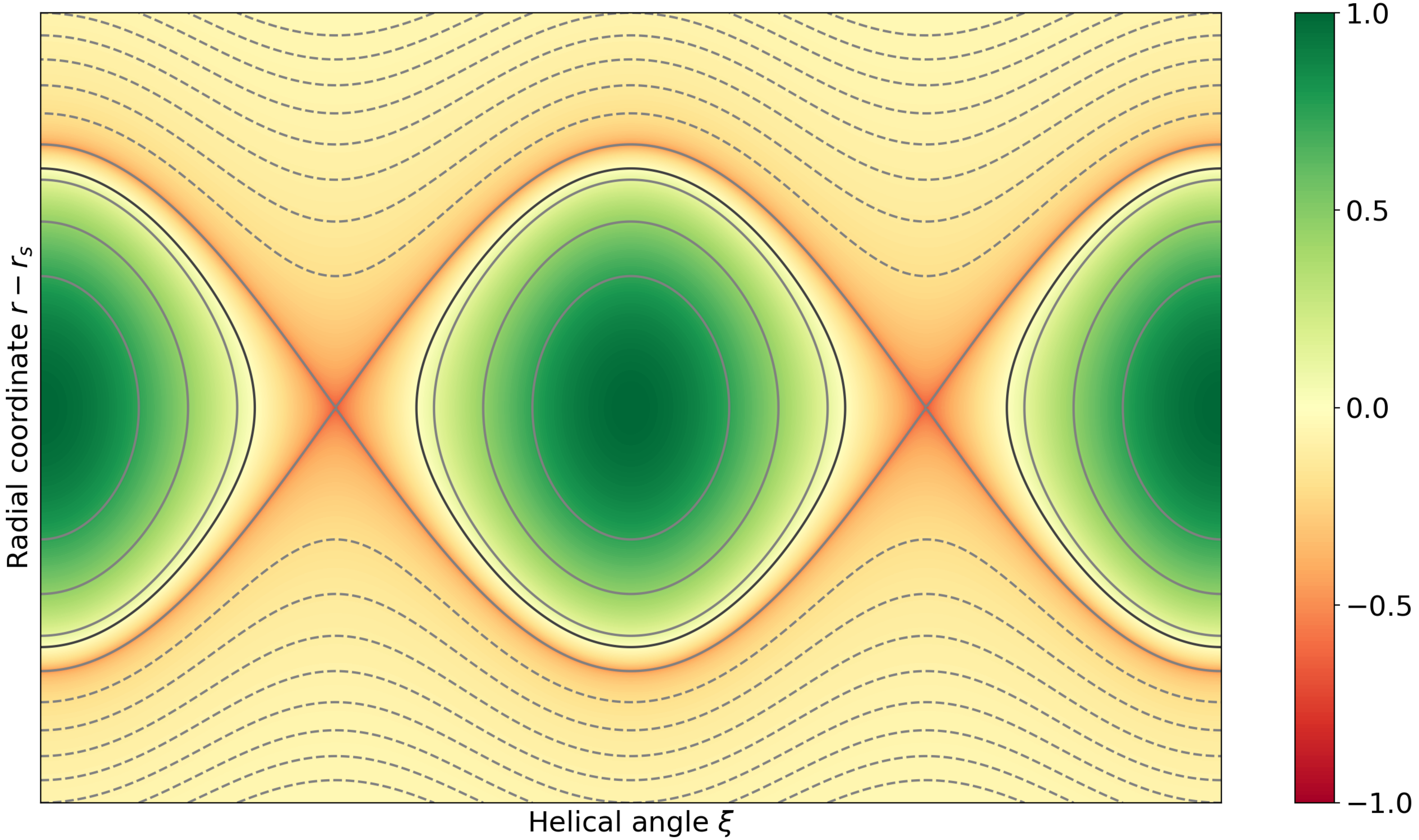

Rotating island, continuous ECCD

Average efficiency: $\langle \eta_{\text{aux}} \rangle = 0.32$

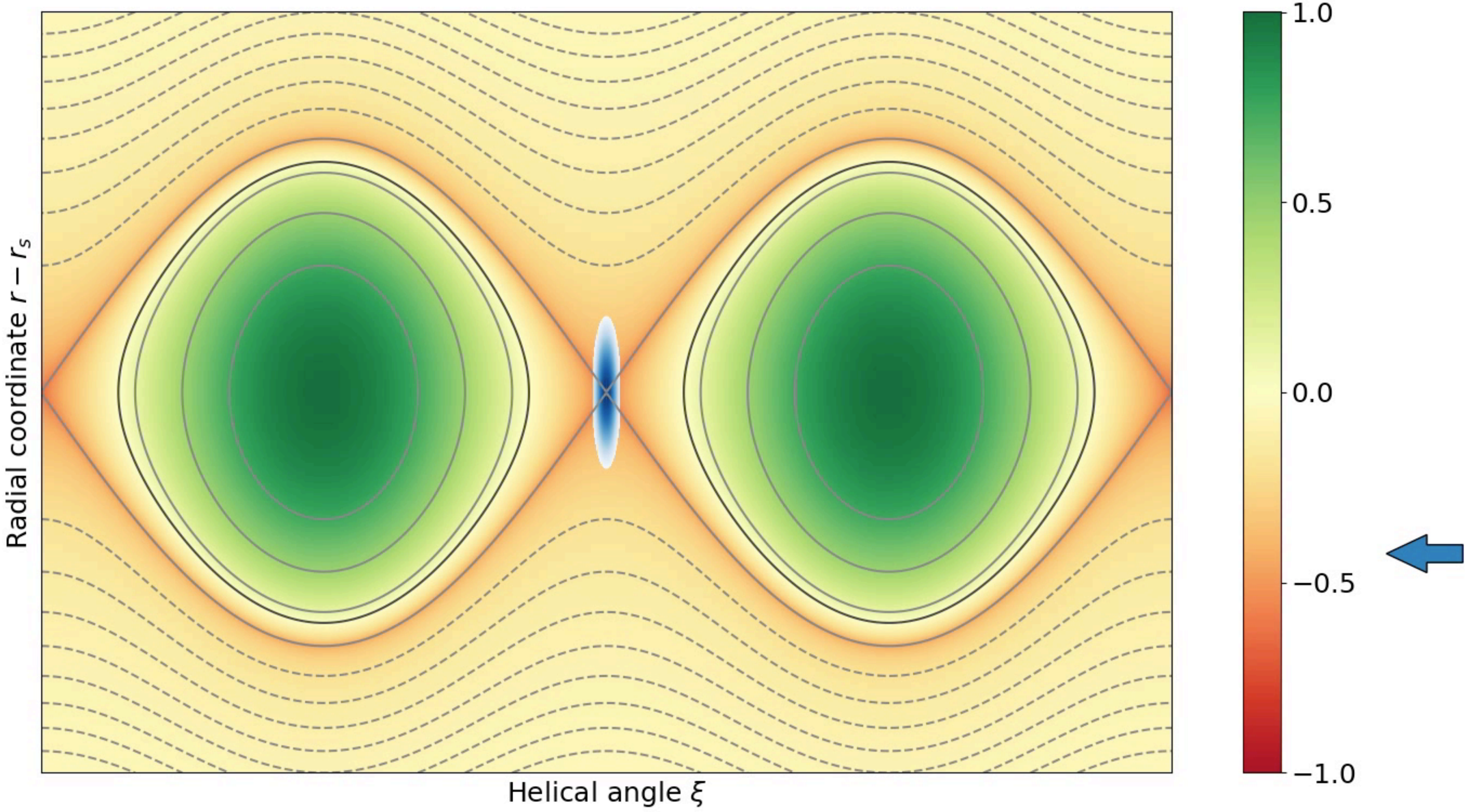

Rotating island, modulated ECCD

Average efficiency: $\langle \eta_{\text{aux}} \rangle = 0.38$

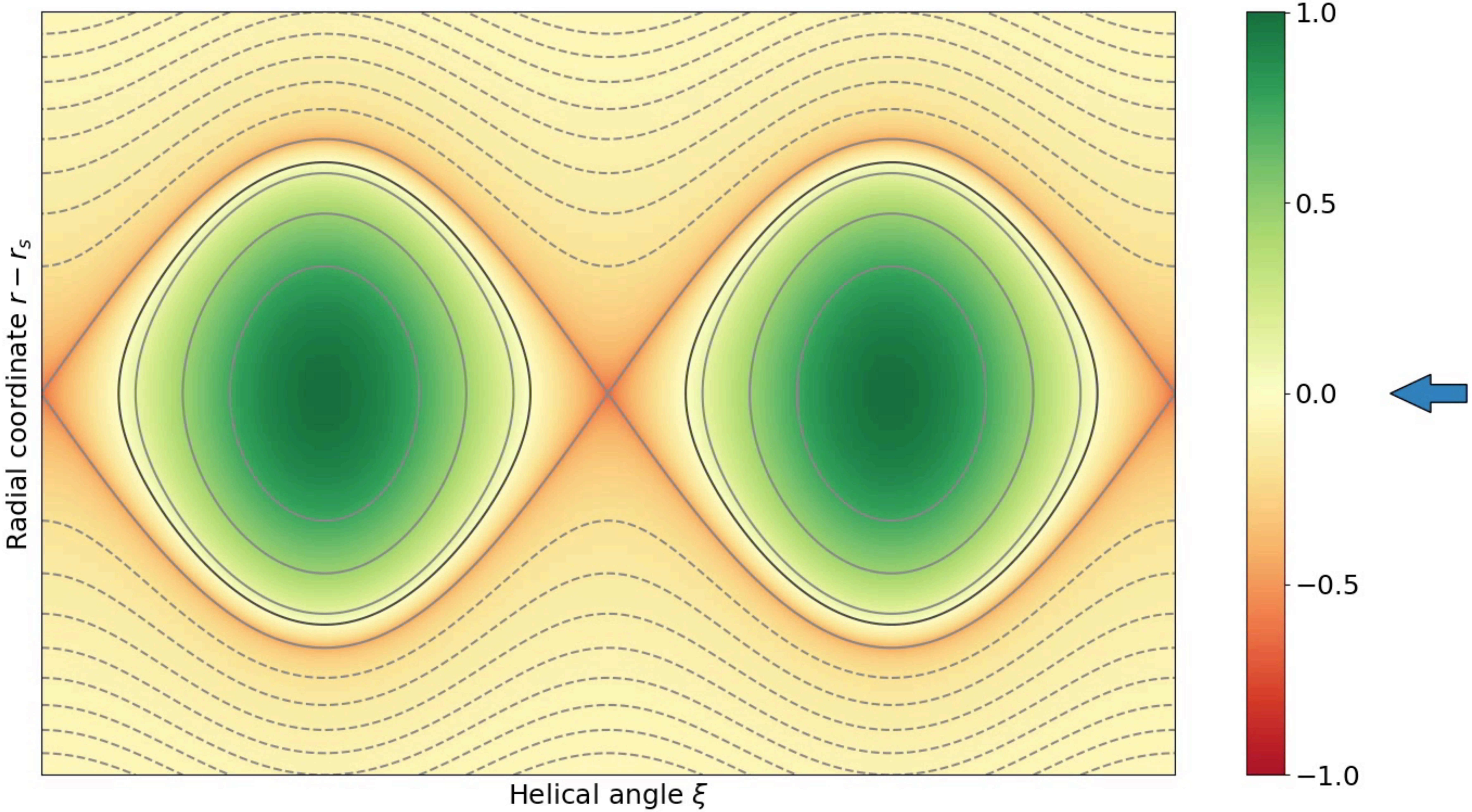

Locked island

Efficiency: $\eta_{\rm aux} = 0.95$

Higher efficiency.
+ larger radial width at O-point reduces sensitivity to misalignment and broadening